

FIRST GLIMPSE RESULTS ON THE STELLAR STRUCTURE OF THE GALAXY

R. A. BENJAMIN,¹ E. CHURCHWELL,² B. L. BABLER,² R. INDEBETOUW,³ M. R. MEADE,² B. A. WHITNEY,⁴ C. WATSON,⁵ M. G. WOLFIRE,⁶ M. J. WOLFF,⁴ R. IGNACE,⁷ T. M. BANIA,⁸ S. BRACKER,² D. P. CLEMENS,⁸ L. CHOMIUK,² M. COHEN,⁹ J. M. DICKEY,¹⁰ J. M. JACKSON,⁸ H. A. KOBULNICKY,¹¹ E. P. MERCER,⁸ J. S. MATHIS,² S. R. STOLOGY,¹² AND B. UZPEN¹¹

Received 2005 April 22; accepted 2005 August 2; published 2005 August 19

ABSTRACT

The GLIMPSE (Galactic Legacy Mid-Plane Survey Extraordinaire) Point Source Catalog of ~ 30 million mid-infrared sources toward the inner Galaxy, $10^\circ \leq |l| \leq 65^\circ$ and $|b| \leq 1^\circ$, was used to determine the distribution of stars in Galactic longitude, l , latitude, b , and apparent magnitude, m . The counts versus longitude can be approximated by the modified Bessel function $N = N_0(l/l_0)K_1(l/l_0)$, where l_0 is insensitive to limiting magnitude, band choice, and side of Galactic center: $l_0 = 17^\circ\text{--}30^\circ$ with a best-fit value in the $4.5\ \mu\text{m}$ band of $l_0 = 24^\circ \pm 4^\circ$. Modeling the source distribution as an exponential disk yields a radial scale length of $H_* = 3.9 \pm 0.6$ kpc. There is a pronounced north-south asymmetry in source counts for $|l| \leq 30^\circ$, with $\sim 25\%$ more stars in the north. For $l = 10^\circ\text{--}30^\circ$, there is a strong enhancement of stars of $m = 11.5\text{--}13.5$ mag. A linear bar passing through the Galactic center with half-length $R_{\text{bar}} = 4.4 \pm 0.5$ kpc, tilted by $\phi = 44^\circ \pm 10^\circ$ to the Sun–Galactic center line, provides the simplest interpretation of these data. We examine the possibility that enhanced source counts at $l = 26^\circ\text{--}28^\circ$, $31^\circ\text{--}34^\circ$, and $306^\circ\text{--}309^\circ$ are related to Galactic spiral structure. Total source counts are depressed in regions where the counts of red objects ($m_k - m_{[8.0]} > 3$) peak. In these areas, the counts are reduced by extinction due to molecular gas, high diffuse backgrounds associated with star formation, or both.

Subject headings: Galaxy: stellar content — Galaxy: structure — infrared: general — infrared: ISM — infrared: stars — ISM: general — stars: general — surveys

1. GLIMPSE AND THE STELLAR STRUCTURE OF THE GALAXY

Since the pioneering work of Kapteyn (1922), star counts have been an important avenue in exploring the stellar structure of the Galaxy. However, progress on understanding the stellar content of the inner Galactic disk has been impeded by dust obscuration of visible light from stars. With the advent of infrared detectors and surveys of increasingly high sensitivity and resolution, significant progress has been made, leading, for example, to strong evidence for a Galactic bar (reviewed by Gerhard 2002).

GLIMPSE, a *Spitzer* Legacy Science Program, has imaged the Galactic plane over Galactic longitudes¹³ $|l| = 10^\circ\text{--}65^\circ$ and Galactic latitudes $|b| \leq 1^\circ$ at 3.6, 4.5, 5.8, and $8.0\ \mu\text{m}$ using IRAC (the Infrared Array Camera; Fazio et al. 2004) on the *Spitzer Space Telescope* (Werner et al. 2004). Angular resolu-

tions range from $1''.4$ at $3.6\ \mu\text{m}$ to $1''.9$ at $8\ \mu\text{m}$. We present the mid-infrared distribution of stars in the Galaxy as determined by GLIMPSE. Properties of the GLIMPSE Point Source Catalog and Archive are summarized in Table 1. Observing strategy, details of source selection, quality flags, and photometric accuracy are provided in the GLIMPSE Science Data Products document (Meade et al. 2005), the GLIMPSE Quality Assurance document (Churchwell et al. 2005), and Benjamin et al. (2003).¹⁴

We have compared the results obtained for all four IRAC bands, explored the effect of using the Archive instead of the Catalog, explored the sensitivity of our results to our faint-magnitude limit, divided the survey region into three latitude strips of $\Delta b = 0^\circ.3$ and considered each strip separately, and experimented with the effect of removing sources with various quality flags. The parameters of all the principal features discussed below remained unchanged.

2. GLIMPSE COUNTS AS A FUNCTION OF LONGITUDE AND LATITUDE

The Catalog and Archive sources were binned into data cubes of $0^\circ.1$ (longitude) $\times 0^\circ.1$ (latitude) $\times 0.1$ mag for all four IRAC bands. The average number of sources in each $0^\circ.1 \times 0^\circ.1$ bin is ~ 1400 for the Catalog and ~ 2200 for the Archive. Figure 1 shows the average number of $4.5\ \mu\text{m}$ sources per square degree in the magnitude range $m = 6.5\text{--}12.5$. The curves indicate the source-count-weighted Galactic latitude distribution, $b_{\text{cen}}(l) = \sum_b N(l, b)b / \sum_b N(l, b)$, which ranges from $b_{\text{cen}} = -0^\circ.05$ to $b_{\text{cen}} = +0^\circ.05$. As $|l|$ increases from 10° to 65° , the counts decrease by a factor of ~ 12 , but there is a pronounced asymmetry between the north and the south in the inner Galaxy. From 10° to 22° , there are $\sim 25\%$ more sources than in the equivalent southern longitude range. There are also apparent enhancements in the counts for $l = 26^\circ\text{--}28^\circ$, $31^\circ\text{--}34^\circ$, and

¹ Department of Physics, University of Wisconsin–Whitewater, 800 West Main Street, Whitewater, WI 53190.

² Department of Astronomy, University of Wisconsin–Madison, 475 North Charter Street, Madison, WI 53706.

³ Department of Astronomy, University of Virginia, P.O. Box 3818, Charlottesville, VA 22903.

⁴ Space Science Institute, 4750 Walnut Street, Suite 205, Boulder, CO 80301.

⁵ Department of Physics, Manchester College, Box 117, 604 East College Avenue, North Manchester, IN 46962.

⁶ Department of Astronomy, University of Maryland, College Park, MD 20742-2421.

⁷ Department of Physics, Astronomy, and Geology, East Tennessee State University, P.O. Box 70652, Johnson City, TN 37614.

⁸ Institute for Astrophysical Research, Boston University, 725 Commonwealth Avenue, Boston, MA 02215.

⁹ Radio Astronomy Laboratory, 601 Campbell Hall, University of California at Berkeley, Berkeley, CA 94720-3411.

¹⁰ School of Mathematics and Physics, University of Tasmania, Private Bag 37, Hobart, Tasmania 7001, Australia.

¹¹ Department of Physics and Astronomy, University of Wyoming, P.O. Box 3905, Laramie, WY 82072.

¹² *Spitzer* Science Center, Mail Stop 314-6, California Institute of Technology, Pasadena, CA 91125.

¹³ Here $|l| \leq 180^\circ$ is the angular distance from the Galactic center.

¹⁴ See <http://www.astro.wisc.edu/glimpse>.

TABLE 1
GLIMPSE CATALOG AND ARCHIVE SOURCE INFORMATION

IRAC BAND	λ^a (μm)	S_0^a (Jy)	A_{IR}/A_K^b	m_{sel}^c (mag)	m_{br}^c (mag)	m_{sens}^d (mag)	CATALOG SOURCES ($\times 10^6$)		ARCHIVE SOURCES ($\times 10^6$)	
							North	South ^e	North	South ^e
1	3.55	277.5	0.56 ± 0.06	14.2	7.0	13.3–13.6	14.775	14.255	21.420	22.044
2	4.49	179.5	0.43 ± 0.08	14.1	6.5	13.3–13.6	14.768	14.250	19.797	19.423
3	5.66	116.5	0.43 ± 0.10	11.9	4.0	11.7–12.3	5.768	5.291	6.095	5.594
4	7.84	63.13	0.43 ± 0.10	9.5	4.0	11.0–12.4	4.426	3.959	4.749	4.268

^a Vega isophotal wavelengths and IRAC zero magnitudes from M. Cohen (2005, unpublished).

^b Extinction from Indebetouw et al. (2005).

^c GLIMPSE Point Source Catalog selection limits and brightness cutoff limits from Meade et al. (2005).

^d The “effective” Catalog sensitivity limit varies over the longitude range $|l| = 10^\circ$ to $|l| = 65^\circ$.

^e The southern Catalog and Archive are still missing $\sim 1\%$ of the survey area.

306° – 309° . Figure 1 also shows contours of the surface density of $\sim 40,000$ unusually red ($m_K - m_{[8.0]} \geq 3.0$) sources using the GLIMPSE and 2MASS catalogs (Cutri et al. 2001). These objects are strongly anticorrelated with the total GLIMPSE counts. The regions of depressed counts coincide with high column densities of ^{13}CO (Simon et al. 2001; R. Shah 2005, private communication) or thermal radio continuum emission (i.e., high-mass star formation).

Figure 2 shows that the number of sources per square degree brighter than magnitude m is well fitted by the first-order modified Bessel function of the second kind, $N(\text{band}, m, |l|) = N_0(|l|/l_0)K_1(|l|/l_0)$, which is expected for an exponential disk population (M. Merrifield 2005, private communication). Our “best-fit” curve excludes data interior to $|l| = 35^\circ$, $l = 306^\circ 5$ – 309° (enhancement), and $l = 301^\circ 5$ – $306^\circ 5$ (missing data). The

inner boundary was varied from $|l| = 25^\circ$ to $|l| = 45^\circ$ to estimate systematic uncertainties due to this choice. The range for all the IRAC bands is $l_0 = 17^\circ$ – 30° . The best fit in the $4.5 \mu\text{m}$ band is $l_0 = 24.2 \pm 0.3$ (random) ± 3.6 (2σ systematic); the slope and level of the fits for the north and south are in marginal agreement. Comparison of this fit with numerical models of a disk population of M and K giants, which are assumed to dominate the source counts (Wainscoat et al. 1992), yields an exponential scale length of $H_* = 3.9 \pm 0.6$ kpc.

For longitudes greater than $|l| = 30^\circ$ and excluding the enhancements mentioned above, the fitting functions for the $4.5 \mu\text{m}$ band predict the observed source densities to within 20% for faint-magnitude cutoffs of 8 and 10 mag, and to within 10% for faint-magnitude cutoffs of 12 and 14 mag. Interior to $|l| = 22^\circ$, the fits overpredict the observed counts by as

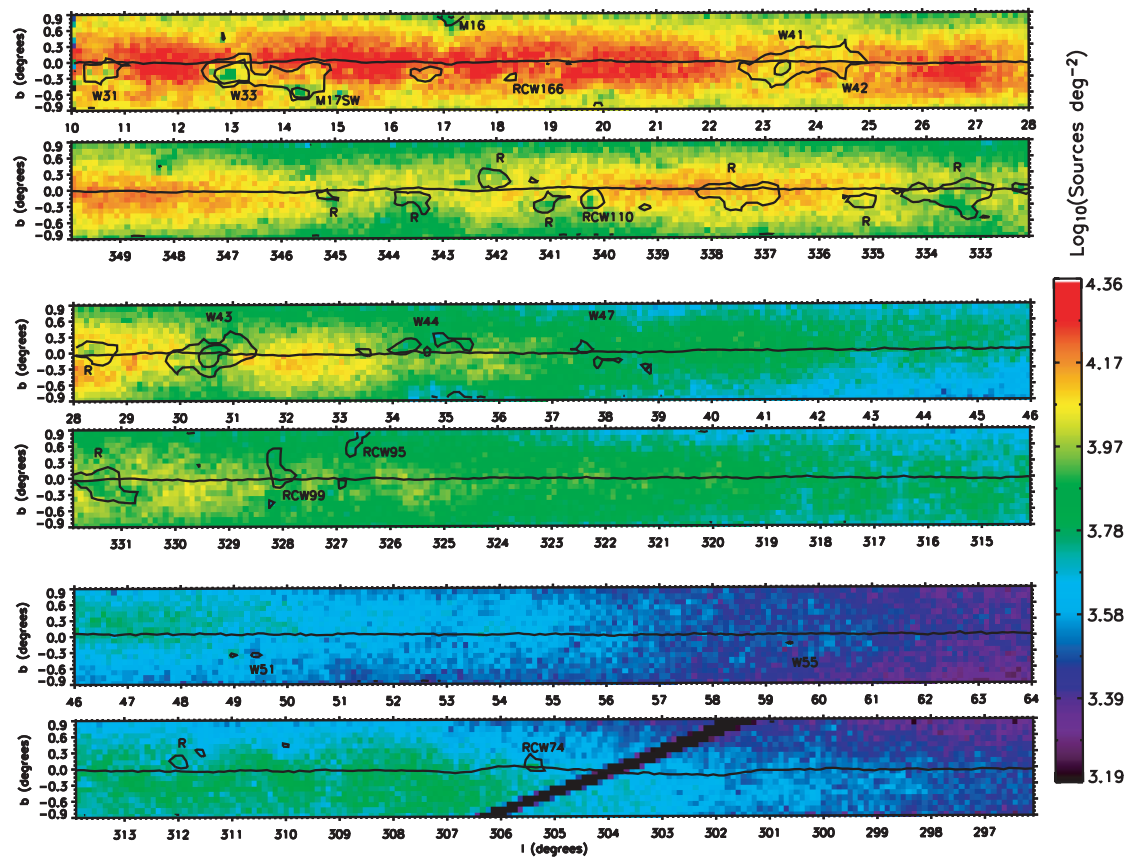


FIG. 1.—The $4.5 \mu\text{m}$ band sources [$\log(\text{sources deg}^{-2})$] from the GLIMPSE Point Source Catalog in the magnitude range $6.5 < m < 12.5$ as a function of Galactic latitude and longitude. Sources have been binned 0.1° (longitude) $\times 0.1^\circ$ (latitude). Notable features include a decline in the number of sources with distance from the Galactic center and a pronounced north-south asymmetry in the inner Galaxy between the north ($l = 10^\circ$ – 22°) and south ($l = 350^\circ$ – 338°). The number of sources is nearly symmetric about the Galactic midplane; the solid lines show the position of the source-count-weighted average latitude. The two contours, $\log(\text{sources deg}^{-2}) = (2.8, 3.3)$, show the surface density of red ($m_K - m_{[8.0]} > 3$) sources; note the anticorrelation with the total counts. These directions are labeled with the corresponding star-forming regions or “R” for strong radio continuum (Altenhoff et al. 1970; Haynes et al. 1978). The dark stripe at $l = 301^\circ$ – 306° is a region of missing data.

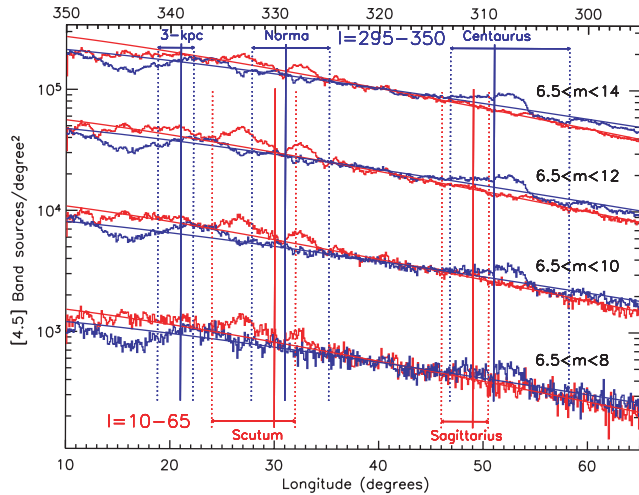


Fig. 2.—Average number of sources per square degree detected by GLIMPSE as a function of longitude in both the northern Galactic plane (*red curves, bottom axis*) and southern Galactic plane (*blue curves, top axis*). Average source densities were obtained by binning the stars into strips of $0^\circ.1$ in longitude and $1^\circ.8$ in latitude. Fits to both curves (see text) over the range $l = 35^\circ - 65^\circ$ (excluding regions of clear enhancements) are also shown. The four sets of curves show the effect of changing the faint-magnitude cutoff. For each drop in magnitude, the number of sources increases by a factor of 3.5 (at 9 mag) to 2.3 (at 13 mag). The vertical lines indicate the estimated directions of spiral arms using different tracers (Engelmaier & Gerhard 1999). The solid lines show their adopted values; the dotted lines indicate the range of published estimates.

much as 30% in both the northern and southern planes. This is not due to confusion, as the drop is independent of the magnitude cut; even at faint magnitudes, we are not affected by confusion (Churchwell et al. 2005).

3. GLIMPSE COUNTS AS A FUNCTION OF MAGNITUDE

Figure 3 shows the number of sources as a function of magnitude for three north-south pairs of directions. Figures 3 and 4 were used to determine the “effective” sensitivity limit, m_{sens} ,

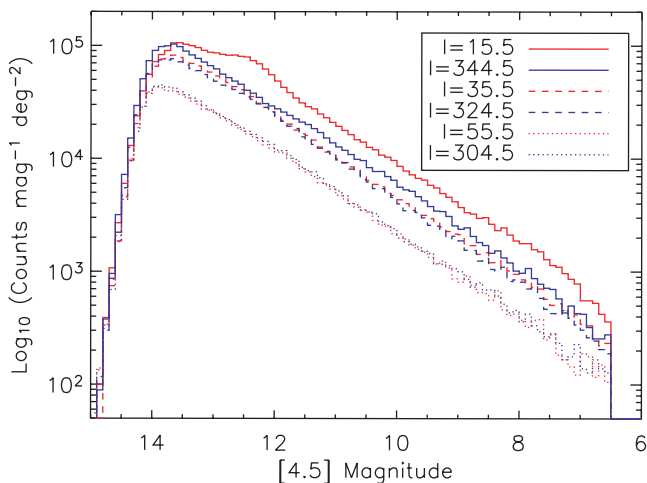


Fig. 3.—Number of sources from the GLIMPSE Point Source Catalog as a function of magnitude for three northern and three southern directions. The outer Galaxy ($l = 55^\circ/304^\circ$) and middle Galaxy ($l = 35^\circ/324^\circ$) curves have approximately the same amplitude and slope. The inner Galaxy ($l = 15^\circ/324^\circ$) shows a significant north-south asymmetry; the northern direction also shows a bump in source counts at a magnitude of $m \sim 12.2$. For all directions shown, the number of sources has been averaged over a 1° (longitude) by $1^\circ.8$ (latitude) region. The Catalog is truncated at 6.5 mag because of detector nonlinearity for sources brighter than this limit.

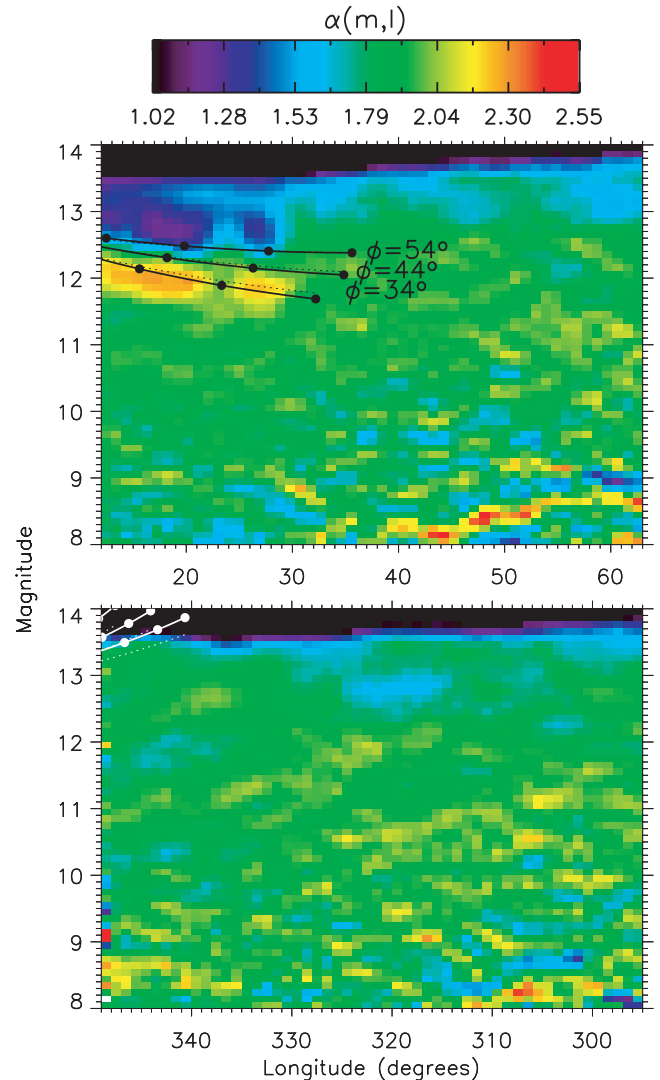


Fig. 4.—Power-law exponent of counts as a function of flux density, plotted as a function of apparent magnitude and Galactic longitude. The position of the ~ 12 mag hump seen toward $l = 15^\circ.5$ in Fig. 3 is seen here to vary consistently in both longitude and magnitude. The locus of magnitude and longitude of a model bar, consisting of stars of absolute magnitude $M_{[4.5]} = -2.15$, foreground extinction $a_{[4.5]}(r) = 0.05$ mag kpc $^{-1}$, and three different position angles ϕ , are shown in black in the top panel and in white in the bottom panel. The circles indicate $R = 3, 4,$ and 5 kpc points along the bar. The dotted lines show the same position angles for zero extinction, with $M_{[4.5]} = -1.8$.

as a function of longitude given in Table 1. The curves shown in Figure 3 can be fitted by $\log n(m) = am + b$. Since $m = -2.5 \log(S/S_0)$, where S is the flux density at magnitude m and S_0 is the flux density for zero magnitude, we can write $N(S) = N_0(S/S_0)^{-\alpha}$, where $N_0 = [2.5/(S_0 \ln 10)] \times 10^b$ sources deg $^{-2}$ Jy $^{-1}$ and $\alpha = 2.5a + 1$. The average $\bar{\alpha}$ over the magnitude range $8 < m < 11$ lies in the range 1.95 to 1.83 for the entire survey area.

Figure 3 shows a “hump” at magnitudes fainter than $m = 12$ in the inner Galaxy toward the north but not the south. This hump is seen in both the Catalog and Archive data in the 3.6 and 4.5 μm bands. It is not detected in the 5.8 and 8.0 μm bands, because of lower sensitivity. To study this further, in Figure 4 we plotted the power-law slope, $\alpha = 2.5d(\log n)/dm + 1$ (with $\Delta m = 0.1$) of the source distribution as a function of Galactic longitude and magnitude. The hump persists over the range $l = 10^\circ - 22^\circ$ and $l = 24^\circ - 29^\circ$. It seems likely that the gap at $l \sim 23^\circ$ is caused by high extinction or high diffuse flux. The central magnitude of the hump at $l = 10^\circ$ is $m_h = 12.5 \pm 0.1$ mag, with a

dispersion of $\sigma_h = 0.25 \pm 0.10$ mag; the amplitude at the peak is 20% above the power-law fit. The shift of the central magnitude of the hump to brighter magnitudes with increasing Galactic longitude is given by $dm_h/dl = -0.025 \pm 0.005$ mag deg $^{-1}$.

4. INTERPRETATION AND COMPARISON WITH PREVIOUS RESULTS

We now summarize the principal features we have found and possible implications for our understanding of Galactic structure. We assume that the distance to the Galactic center is $R_0 = 8.5$ kpc.

Exponential disk.—For $|l| \geq 22^\circ$, the counts in all four IRAC bands can be fitted by $N(\text{band}, m, |l|) = N_0(|l|/l_0)K_1(|l|/l_0)$. For the 4.5 μm band, the best fit (excluding regions of obvious enhancement) yields $l_0 = 24.2 \pm 3.6$ (systematic). For all four IRAC bands and for several magnitude cutoffs, we find that $l_0 = 17^\circ\text{--}30^\circ$. This can be compared with our results obtained by binning the 2MASS *K*-band sources in an identical fashion, which yields $l_{\text{sc}} > 40^\circ$. Presumably this larger number is due to higher extinction in the *K* band. Converting this angular scale length to a radial scale length requires modeling of the spatial distribution of stars, the infrared luminosity function, and extinction (Cohen 1993). Preliminary modeling indicates that the majority of our sources are M giants and late K giants and yields a radial scale length for the exponential disk of $H_* = 3.9 \pm 0.6$ kpc. Interior to $|l| = 22^\circ$ there are $\sim 20\%$ fewer sources than predicted by this fit, which may indicate a stellar “hole” (or more accurately, deficit) interior to Galactocentric radius $R_h = 3.2 \pm 0.3$ kpc. This is comparable to $R_h = 2.9\text{--}3.3$ kpc, derived from COBE DIRBE data (Freudenreich 1998).

Galactic bar.—We see a strong north-south asymmetry in counts for $|l| \leq 30^\circ$, with $\sim 25\%$ more sources in the north and a distinct hump in the number of stars at apparent magnitude $m \sim 12.5$ over the longitude range $l = 10^\circ\text{--}30^\circ$. Both these facts suggest that we have detected the Galactic bar. Estimates for the bar’s orientation (relative to the line connecting the Sun to the Galactic center) typically range from $\phi = 15^\circ$ to $\phi = 35^\circ$ (Gerhard 2002). If the “hump” seen in Figures 3 and 4 is due to stars in the bar with a well-defined peak at constant absolute magnitude, we can estimate the bar’s orientation and length. In Figure 4, we have plotted the magnitude and longitude expected for a linear bar in the plane of the Galaxy passing through the Galactic center with a foreground extinction $a_{[4.5]}(d) = 0.05$ mag kpc $^{-1}$, using the fiducial $a_v(d) = 1$ mag kpc $^{-1}$ (Mihalas & Binney 1981), $A_v/A_K = 8.8\text{--}7.5$ (Cardelli et al. 1989), and $A_{[4.5]}/A_K = 0.43$ (Indebetouw et al. 2005). The best fit to the data yields $\phi = 44^\circ \pm 10^\circ$, $R_{\text{bar}} = 4.4 \pm 0.5$ kpc, and $M_{[4.5]} =$

-2.15 ± 0.2 mag; the effect of increasing extinction is to increase ϕ and M . Fitting the data with zero extinction yields $M_{[4.5]} = -1.8$ mag. The requirement that $M_{[4.5]} = -2.15$ mag to match the data suggests that the hump is due to K2–K3 giants (Cohen 1993; Hammersley et al. 2000). Figure 4 shows that the predicted m_{hump} for the model bar falls below our sensitivity limit at $l = 350^\circ$, but the observed increase in counts seen in Figure 1 from $l = 345^\circ$ to $l = 350^\circ$ is consistent with our derived bar length. Although a bar seems to be the simplest interpretation of these results, other configurations should be explored.

Stellar enhancements/spiral arms (?).—Outside $l = 22^\circ$, we find three regions where counts are 20% higher than the exponential fitting functions. These are at $l = 26^\circ\text{--}28^\circ$, $31.5^\circ\text{--}34^\circ$, and $306^\circ\text{--}309^\circ$. It is tempting to associate these features with spiral arm tangencies. The presence of the “hump” in the $l = 26^\circ\text{--}29.5^\circ$ region argues that it is a continuation of the same structure observed from $l = 10^\circ$ to $l = 20^\circ$, complicated by the presence of extinction. Unresolved questions regarding extinction also affect interpretation of the $31^\circ\text{--}34^\circ$ feature. The third feature could be identified with a previously known spiral arm tangency (Centaurus, $l \sim 309^\circ$). No plausible enhancement in star counts is seen toward the Sagittarius spiral arm tangency at $l \sim 49^\circ$.

Extinction/diffuse background.—There is a clear anticorrelation between the GLIMPSE Catalog counts and the counts of sources with $m_K - m_{[8.0]} > 3.0$ in certain regions (shown in Fig. 1). Counts can be depressed by either increased extinction or high diffuse background, both of which are associated with star-forming regions and molecular clouds. It is clear that the effects of extinction and diffuse emission on the source counts deserve future scrutiny. For this reason, the parameters of the structures discussed here should be considered preliminary.

Many of the principal structures seen in this work have been detected or hinted at in previous infrared investigations. What differentiates the GLIMPSE results from these previous works is the uniform and complete sampling of the Galactic plane at $\leq 2''$ resolution, the significantly reduced extinction in the mid-infrared, and the very large sample of GLIMPSE sources. Even without any color selection of our sources, we find that we are able to detect and confirm several fundamental Galactic structures.

We thank the referee, Stephan Jansen, Mike Merrifield, Paul Rybski, and Ronak Shah for help and suggestions, and we acknowledge support for this program through NASA contracts 1224653, 1224653, 1225025, 1224681, 1224988, 1259516, 1253153, and 11253604 by the Jet Propulsion Laboratory, Caltech, under NASA contract 1407. We also gratefully acknowledge use of data products from the Two Micron All Sky Survey.

REFERENCES

- Altenhoff, W. J., Downes, D., Goad, L., Maxwell, A., & Rinehart, R. 1970, *A&AS*, 1, 319
- Benjamin, R. A., et al. 2003, *PASP*, 115, 953
- Cardelli, J. A., Clayton, G. C., & Mathis, J. S. 1989, *ApJ*, 345, 245
- Churchwell, E., et al. 2005, GLIMPSE Quality Assurance Document (Madison: Dept. Astron., Univ. Wisconsin)
- Cohen, M. 1993, *AJ*, 105, 1860
- Cutri, R. M., et al. 2001, Explanatory Supplement to the 2MASS Second Incremental Data Release (Pasadena: Caltech)
- Englmaier, P., & Gerhard, O. 1999, *MNRAS*, 304, 512
- Fazio, G. G., et al. 2004, *ApJS*, 154, 10
- Freudenreich, H. T. 1998, *ApJ*, 492, 495
- Gerhard, O. 2002, in *ASP Conf. Ser. 273, The Dynamics, Structure, and History of Galaxies*, ed. G. S. Da Costa & H. Jerjen (San Francisco: ASP), 73
- Hammersley, P. L., Garzón, F., Mahoney, T. J., López-Corredoira, M. & Torres, M. A. P. 2000, *MNRAS*, 317, L45
- Haynes, R. F., Caswell, J. L., & Simons, L. W. J. 1978, *Australian J. Phys. Astrophys. Suppl.*, No. 45
- Indebetouw, R., et al. 2005, *ApJ*, 619, 931
- Kapteyn, J. C. 1922, *ApJ*, 55, 302
- Meade, M. R., et al. 2005, GLIMPSE Legacy Science Data Products (ver. 1.5; Madison: Dept. Astron., Univ. Wisconsin)
- Mihalas, D., & Binney, J. 1981, *Galactic Astronomy* (2nd ed.; San Francisco: Freeman)
- Simon, R., Jackson, J. M., Clemens, D. P., Bania, T. M., & Heyer, M. H. 2001, *ApJ*, 551, 747
- Wainscoat, R. J., Cohen, M., Volk, K., Walker, H. J., & Schwartz, D. E. 1992, *ApJS*, 83, 111
- Werner, M. W., et al. 2004, *ApJS*, 154, 1